



AIAA 2002-1200

**THE EFFECT OF GEOMETRIC SCALE
ON THE CONFIGURATION OF A
SOLAR SAIL**

Peter D. Washabaugh

Department of Aerospace Engineering
University of Michigan
Ann Arbor, MI 48109-2140

**43rd Structures, Structural Dynamics,
and Materials Conference:**

3rd Gossamer Spacecraft Forum

22-25 April 2002
Denver, CO

The Effect of Geometric Scale on the Configuration of a Solar Sail

Peter D. Washabaugh[†],

University of Michigan
Ann Arbor, Michigan 48109-2140

ABSTRACT

Various configurations and geometric scales of solar sails are compared with alternate advanced propulsion technologies. The study illuminates certain critical parameters such as the specific stiffness of the structure, a minimum area density, a minimum 'smoothing stress', and a need for long duration missions (e.g. > 100 days). As the thrust requirement increases, the geometric scale of the sail increases, and the optimal configuration varies from a simple plate, to a stiffened radial rib topology. As the scale increases further, a rotating oblate ellipsoid that is inflated is the preferred configuration. As a first step toward substantiating some of the parameters chosen in this study some initial experiments were performed to determine some properties of membrane materials. These include surface reflectivity measurements using interferometers as a function of membrane stress. One consequence of using a solar sail propulsion technique is that to minimize the support mass, the payload and bus components are naturally driven toward a distributed layout. A limiting feature of sail's propulsion capability is its inherently high compliance. There is strong coupling between the structural shape and the thrust performance and this leads to potentially large uncertainties in navigational parameters such as position

INTRODUCTION

Solar sails are a potential means to efficiently obtain large changes in velocity with the notable feature of using no propellant.^{1,2} Sails are typically portrayed as being reinforced membrane structures. For example Figure 1 is a solar sail configuration which consists of a membrane that is reinforced with radial ribs. It is necessary to keep the membrane in tension to provide a smooth surface³. The radial ribs are under compression. The compressive load is used to place the overall membrane in tension. The ribs and membrane together are self-equilibrating.

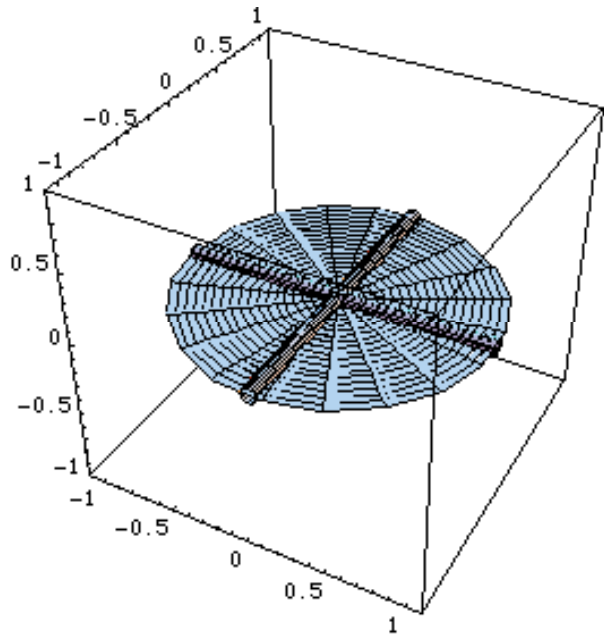


FIGURE 1: A schematic of a solar sail consisting of a membrane and four radial ribs.

[†] Associate Professor of Aerospace Engineering

Copyright © 2002 by Peter D. Washabaugh. Published by the American Institute of Aeronautics and Astronautics, Inc. with permission.

Thrust is obtained by the reflection of light off a large area. The properties of the reflecting surface are critical to the solar sail performance. A diffusive surface (i.e. surface roughness on the order of the wavelength of the reflected light) would impact efficiency in that rather than reflecting light in a single direction, light would be

scattered in many directions. Similarly if the surface is not smooth (i.e. surface irregularities with features significantly greater than the wavelength of light), the light would again be reflected in numerous directions rather than a single one. Thus the surface smoothness of the membrane both at small and large scales can impact the performance of the sail as a propulsion device.

An intriguing aspect to solar sails is that in order to obtain any appreciable acceleration (i.e. 1 mm/s^2), they need to have low mass and simultaneously large thrust they need to be huge, (e.g. 100's of meters in lateral size or even larger). One consequence of this size and mass restriction is that these structures would have low fundamental natural frequencies (e.g. 10's of mHz or lower). In other words, in order to minimize the mass of the propulsion system, the structural mass would be minimal and thereby the structure would be flexible. Motion in the structure would impact the thrust performance. For example during a maneuver the craft will likely vibrate thereby causing the reflective surface to change shape and result in a moving thrust vector.

The purpose of this investigation is to place bounds on some of the gross features of a solar sail. In particular the local smoothness of likely solar sail reflector materials are studied experimentally. Sail configurations are studied analytically and their performance in terms of maximum acceleration is compared. This maximum acceleration can be compared with other propulsion technologies such as Solar Electric Propulsion (SEP).

From this investigation, an initially crumpled membrane material can be smoothed if a sufficiently high in plane stress is applied. The best acceleration is obtained by different configurations, depending on the scale of the sail. These configuration range from a simple un-reinforced and un-stretched "membrane" at small scales, to a reinforced membrane at intermediate scales and an inflated structure at large scales.

LOCAL SMOOTHNESS

The local smoothness of candidate membrane materials were studied experimentally. The materials consisted of Mylar membrane that were both uncoated and aluminized. The membranes had thickness of 5, 7.5 and 10 micrometers. The

membranes were cut into disks approximately 150 mm in diameter and were crumpled by hand into small balls to simulate packaging. The membranes were then stretched on a 100 mm diameter aluminum ring mandrel until a smooth surface was obtained. The transition from being rough to smooth was quite dramatic.

Once a smooth membrane was obtained, some of its properties were measured. The gross surface profile was measured using a Zygo interferometer. For the aluminized Mylar the membrane was just like any other mirrored surface, with the exception that room noise needed to be minimized to keep the membrane from moving (the membrane acts like a microphone). The transparent material was tested by transmitting the incident plane wave of light from the instrument, through the material, off a flat test mirror, back through the membrane material for a second time and then back into the interferometer. Some of the aluminized samples were further tested in a Wyco phase shifting interferometer with the intent of detecting small scale surface roughness and delamination of the aluminum coating⁴.

Figures 2a and 2b show some typical results from the Zygo interferometer, Figures 3a and 3b show some typical results from the Wyco interferometer. Both instruments showed that even though the aluminized membrane material was abused by crumpling, the residual surface roughness was less than +/- 55 nanometers while in a sufficiently large tensile state. It is important to note that the two measurements were over disparate lateral scales and used different techniques. The Zygo interferometer used an aperture of approximately 75 mm diameter. The wave-front of light was distorted by the shape of the supporting mandrel. The mandrel was not optically flat. The surface roughness was obtained by measuring the distorted wave-front and removing the first five low order aberrations (tilt, focus, astigmatism, coma and spherical). The surface roughness is what remains after these aberrations have been removed. The Wyco interferometer is a more direct measurement however over a much smaller scale. It was configured to measure the surface roughness over an approximately 1mm by 1mm square area. The results from the Zygo interferometer for a transparent membrane were interesting in that they showed marked striations (e.g. see Figure 2b). These striations are likely inherent to the material in that the crimping was on a significantly smaller scale.

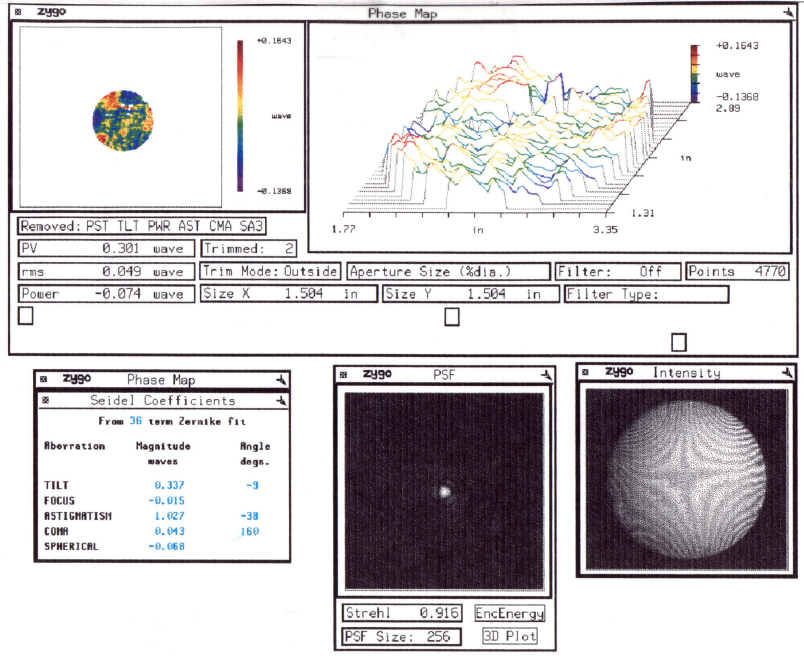


FIGURE 2A: Typical results from a Zygo interferometer measurements of a 5 micrometer thick aluminized Mylar membrane, stressed to approximately 10^7 Pa tensile stress.

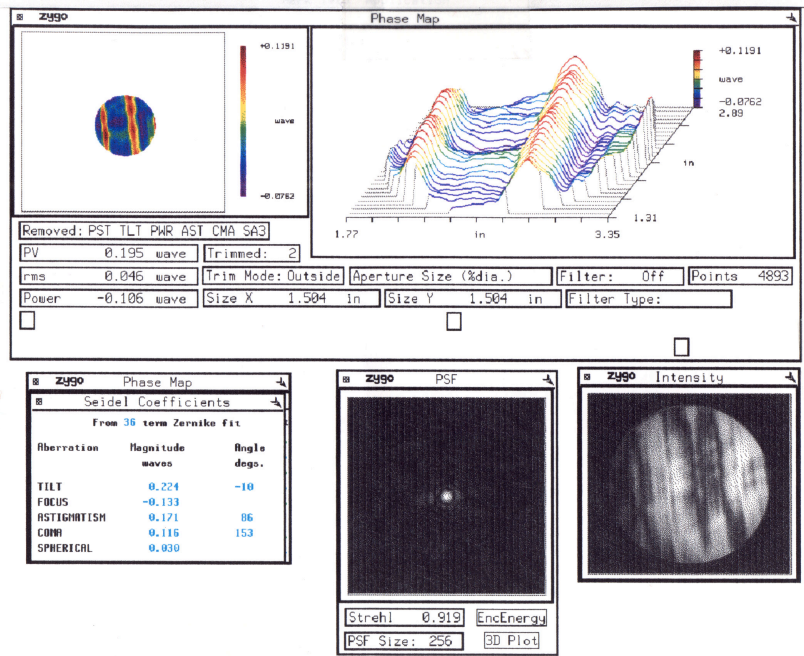


FIGURE 2B: Typical results from a Zygo interferometer measurements of a 5 micrometer thick transparent Mylar membrane, stressed to approximately 10^7 Pa tensile stress.

MEM-3 09:25 06/22/95 TC 10.5x
 RMS: 15.8nm SURFACE WVLN: 631.5nm
 RA: 12.1nm Masks: None R Crv: -28.64m
 P-V: 127nm

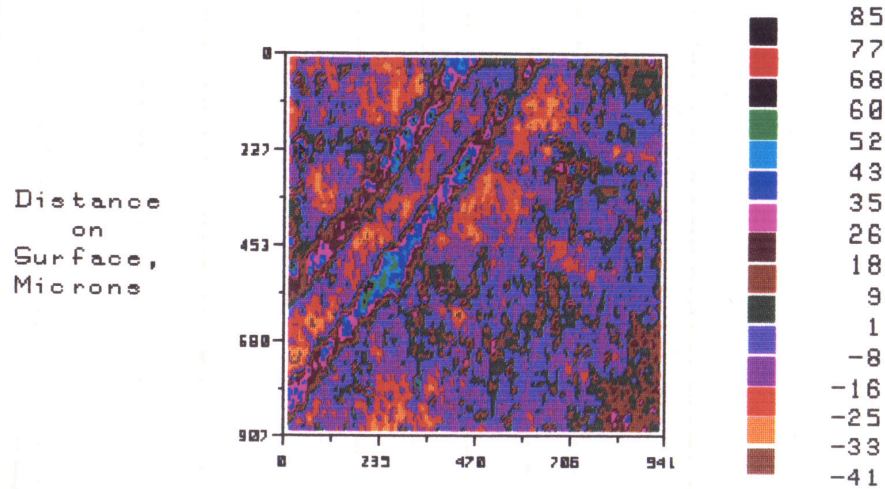


FIGURE 3A: Typical Wyco interferometer results of a 5 micrometer thick aluminized Mylar membrane.

MEM-3 09:25 06/22/95 TC 10.5x
 RMS: 15.8nm HISTOGRAM WVLN: 631.5nm
 RA: 12.1nm SURFACE R Crv: -28.64m
 P-V: 127nm

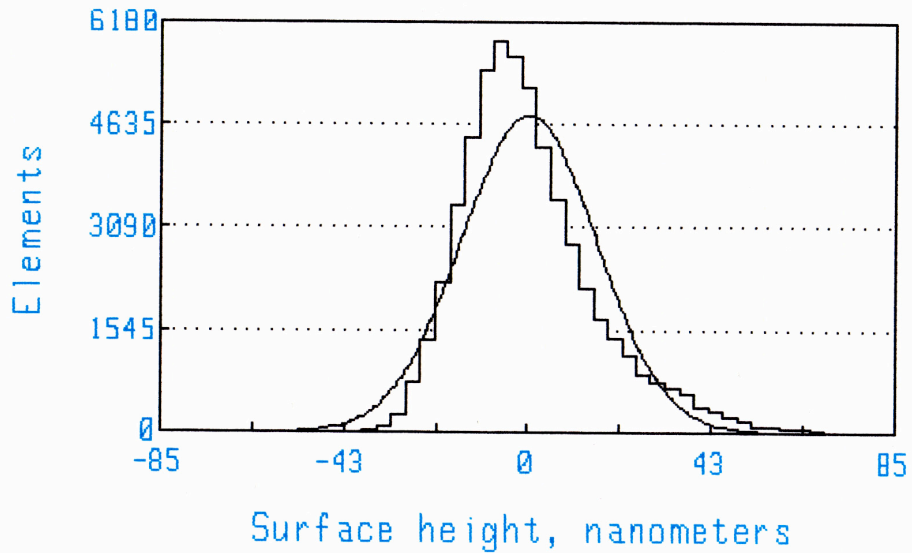


FIGURE 3B: Histogram of the surface roughness of the measurement shown in Figure 3a.

The tension in the membrane was estimated by measuring the first two natural frequencies with symmetric modes. The symmetric modes were obtained because the membrane was acoustically excited⁵. Talcum powder on the surface would indicate the mode by collecting along nodal curves. Since this test was somewhat destructive – in that it contaminated the surface – this measurement was done after the optical surface measurements. The membranes appeared to be smooth consistently at stresses of approximately 10^7 Pa.

These tests are preliminary. It would be more compelling to track the surface roughness as function of stress. However, they do demonstrate that membranes are resilient and even after abuse can be smoothed into acceptable optical surfaces. This smoothing appears to be the consequence of the inherent structural properties of the membrane in that to first order, the membrane has no bending stiffness⁵. Thus the effects of residual stress as a result of the crimpling is significantly diminished. This is an encouraging result in that the membranes can be packaged in almost any fashion and still be useable. It is important to note that the stress reported here is an upper bound. If the membrane is annealed, or if the membrane is pampered the smoothing stress will likely be lower. However this speculation needs to be substantiated with further tests. These tests also illustrate the importance of boundary flatness. It is not surprising that the out-of-flatness of the boundary resulted in an out-of-flat membrane. Other tests should be done on sub-micron thick Mylars with area densities of less than 3 g/m^2 .

SAIL CONFIGURATIONS

Since materials with acceptable local properties are available a next step is to ascertain some of the global properties of the materials as they are used in various sail configurations. Four types of configurations are considered. These are illustrated in Figures 4a, through 4d. They are a plate, a radially stiffened membrane, a toroidally stiffened membrane and a membrane in the shape of an ellipsoid.

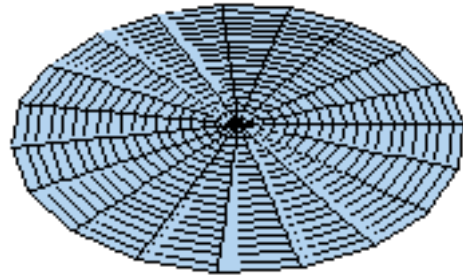


FIGURE 4A: A circular plate initial configuration.

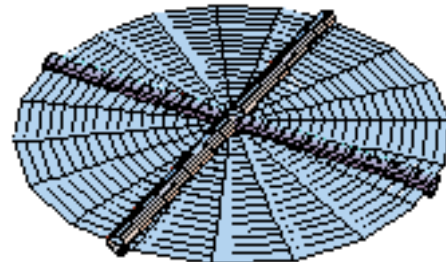


FIGURE 4B: A circular membrane initial configuration reinforced with compressive ribs to maintain tension.

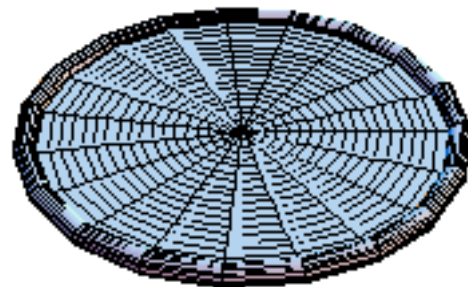


FIGURE 4C: A circular membrane initial configuration reinforced with a peripheral compressive toroid to maintain tension.

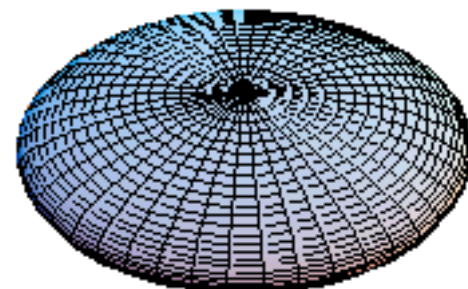


FIGURE 4D: An ellipsoidal membrane initial configuration inflated to maintain tension.

The “plate” configuration resists deformation simply due to the bending stiffness of material⁷. That is, the material is not under tension. The other configurations have surfaces that are under a tension of 10MPa. The ribbed configuration is sized so that the ribs are under compression and have a cross-section that is sufficient to avoid buckling⁷. Similarly, the toroidal configuration has a toroid that is under compression because it is keeping the membrane under tension. This toroid also has a sufficiently large cross-section to avoid local and global buckling⁸. The ellipsoid uses pressure to maintain tension in the membrane. Its aspect ratios are fixed to be a critical Jacobi ellipsoid because it is the most oblate ellipsoid that can be gravitationally stabilized under rotation⁹.

SAIL DEFORMATION

The loading on these structures can be straightforwardly determined from first principles⁶. The structures were assumed to be at a constant 1 AU from the sun. The sun is assumed to be a black radiator at 5777 K. This results in a solar insolation constant of 1.3 kW/m² which corresponds to a spectrum of photons at a flux of 3×10^{26} photons/(m²s).

The momentum of a photon is the energy of the photon divided by the speed of light. Thus to obtain an equivalent pressure acting on the surface one needs to ascertain how the momentum vector is altered by the surface for each photon. This process is illustrated in Figure 5.

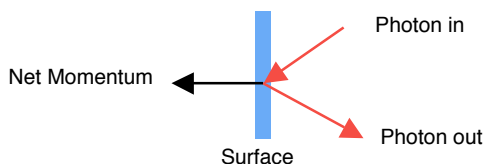


FIGURE 5: Photons imparting momentum to a surface.

A photon that glances off a surface (i.e. does not change its direction) does not impart any momentum. This occurs when the surface normal is perpendicular to the photon’s propagation direction. A photon that gets its propagation direction rotated by 180⁰, i.e. it propagates back toward its original location, imparts the most momentum. This momentum is two times the photon’s momentum. This occurs when the surface normal is parallel to the propagation

direction. In this later case, if you integrate up all the photons acting at 1 AU, the equivalent pressure acting on the surface is approximately 10 μNewtons/m².

At small scales, this solar pressure is so small that the bending stiffness of the membrane – even for sub-micron thicknesses – is sufficient for structural support. Assume that the structure is supported at its center. This assumption would be valid if the payload mass was concentrated at the center, e.g. the spacecraft bus. Further, assuming that the structure has its thickness fixed at its minimum thickness (1 μm), at very small radii (say 1 mm) the structure is sufficiently stiff to maintain its shape in the presence of the tiny solar pressures. The deformed shape is shown in Figure 6a. This shape is indistinguishable from the initial shape shown in Figure 4a.

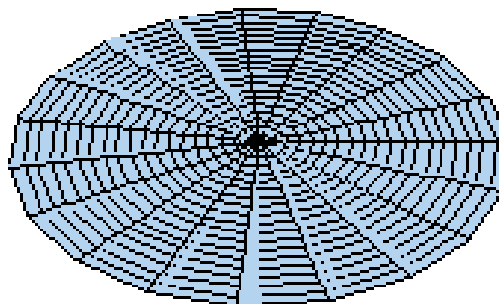


FIGURE 6A: DEFORMED PLATE WITH A RADIUS OF 1MM.

However, as the radius the configuration is increased while keeping the membrane thickness constant, the bending loads accumulate. That is, the small solar pressures are integrated over the surface. If the surface is sufficiently large, the even a small pressure can provide a large force. This force is concentrated on the payload mass – which in this scenario is located at the center. The deformed configuration for a larger scale plate is shown in Figure 6b. The deformation of the plate in the deformed configuration is now readily apparent.

If the radius of the configuration is increased further (still keeping the thickness constant) the deformation becomes even more pronounced. The deformed configuration of a plate with a 5 m radius is shown in Figure 6c.

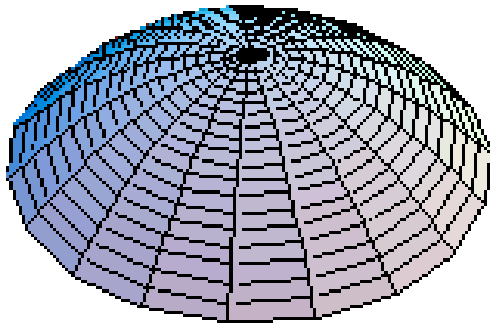


FIGURE 6B: Deformed plate with a radius of 0.5m

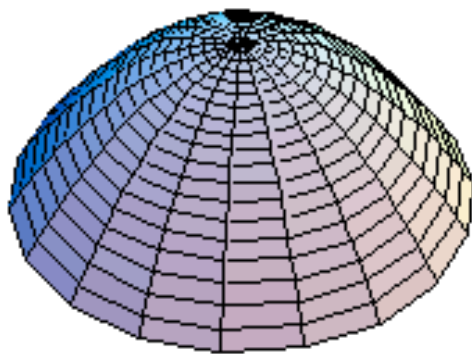


FIGURE 6C: Deformed plate with a radius of 5 m

The importance of the deformed configuration is that the larger the configuration, the less effective the propulsive capability of the sail. The material near the periphery necessarily has a surface normal that is NOT aligned with the incident photons. This angle increases with radius.

The deformations described above are merely estimates provided by linear plate theory⁷. Linear plate theory only applies for small deformations and the deformations shown in figures 6b and 6a are definitely large. However, as will be described in the remainder, once the structure starts to deform appreciably (as its size is increased), its performance as a propulsion device begins to suffer. The interest here is the performance of the system while it is still in a linearly deformed range, and the scales at which it begins to lose performance.

Similar calculations can be accomplished for the other configurations (e.g. rib, torioid and the ellipsoid). The deformation of the ribbed system is approximated by all of the loads being transferred

to the ribs. The bending is found using simple Bernoulli-Euler beam theory¹⁰. The toroidal configuration's deformation is approximated by the deformation of a circular membrane⁵. The deformation of the ellipsoid can also be approximated by membrane equations with the added stiffness of a backing pressure¹¹. In all cases the payload is assumed to be centrally located. Consequently, as the scale of the structure is increased, with certain parameters held constant (e.g. membrane thickness, membrane stress), the structures eventually all bend as shown in Figure 6c.

It is important to recognize that these calculations are preliminary in that interactions between the deformed configuration and the loading have not been fully investigated. For instance the ribs are designed in their initial configuration to be buckling limited, yet when the transverse solar pressure is applied the ribs are no-longer straight. Since they are under compression there will be interaction between the solar pressure loading and the axial loading. However it turns out that this is a problem that does not need to be addressed, at least here, because under these optimistic assumptions the radial reinforced configuration has less impressive performance than other configurations. Any additional mass to stiffen the ribs system and alleviate this interaction would only worsen the performance.

Perhaps more importantly there is no interaction between the load and the deformation. The total load that deforms the structure, L , is always the pressure times the area. That is, this load assumes that the structure is in its initial configuration where the reflective surface normal is always parallel to the incoming light. However the available thrust, T , takes into account the deformation of the reflective surface. The reflective surface has a surface normal parallel to the incoming light at the center-but at the periphery of the structure it can deviate substantially. Consequently T is always less than L . A better calculation would be to perform an iteration and use the loads calculated in the thrust, to be the next applied load to thereby determine a refined deformation (e.g. this is done in aeroelasticity¹⁰).

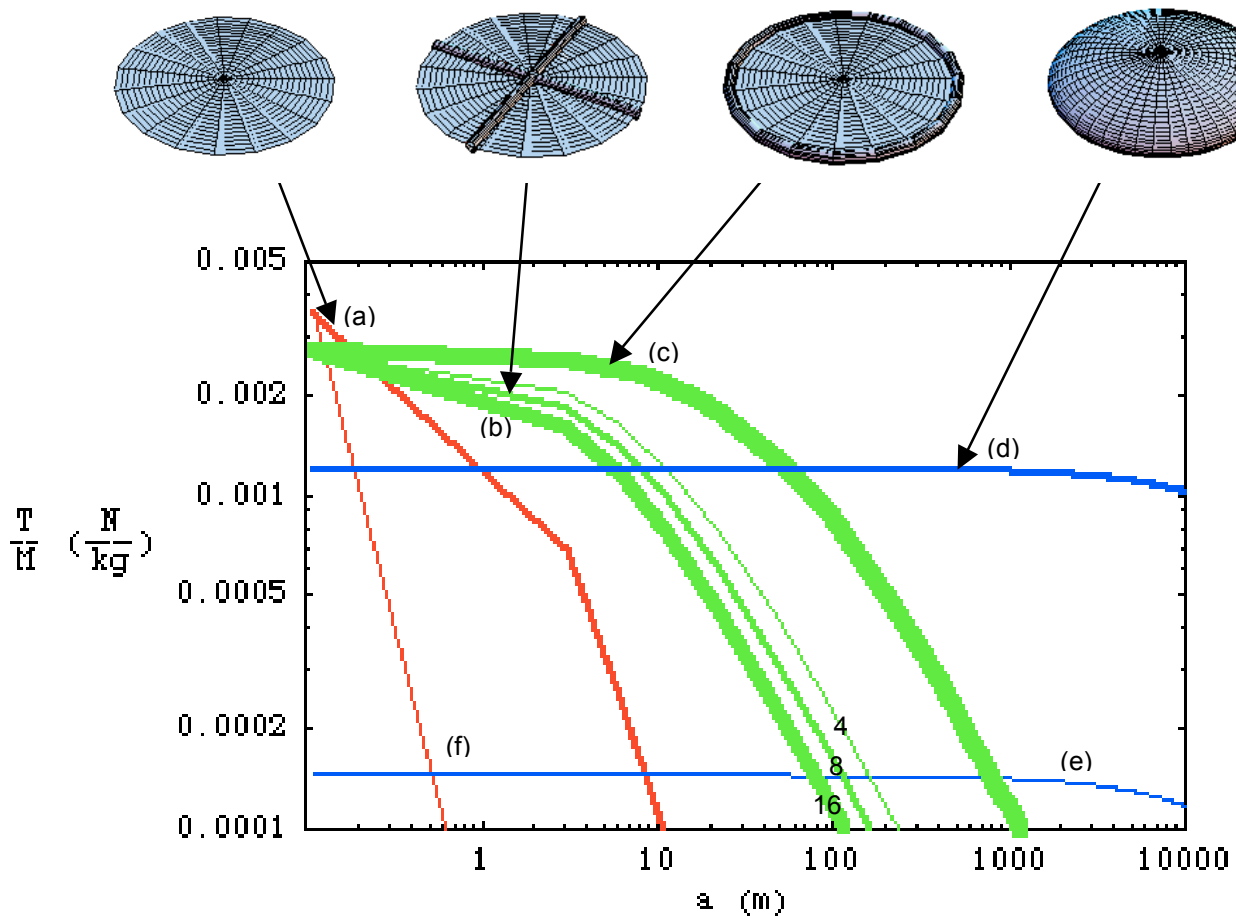


FIGURE 7: A comparison of the acceleration performance of the various configurations as a function of size. (a) Plate, (b) Reinforced using 4, 8, 16 Ribs (c) Toroid, (d) Critical Jacobi Ellipsoid, (e) Sphere (f) Collapsed 1/10 thickness plate. The base membrane is $1\mu\text{m}$ thick mylar, with the reinforcement as described in the text. The solar pressure is $10\mu\text{Pa}$ approximating performance at 1 AU

SAIL PERFORMANCE

The thrust available on the structure can be divided by the mass of the structure to obtain an acceleration of the craft. A summary of this calculation as a function of size, and for each configuration is shown in Figure 7.

This result has some interesting features and needs some explanation. First, the maximum acceleration is obtained by the plate configuration because it consists of a single minimal thickness surface. The maximum acceleration is approximately 4 mm/s^2 . This number can be increased by simply choosing a thinner material.

As the diameter of this single surface is increased it begins to have substantial deformation. This deformation results in a loss of thrust performance. Consequently, once the diameter gets above approx 0.2 m, added material simply goes to waste. Some type of reinforcement is needed to keep the surface from bending.

The single surface was reinforced in two ways. The first way was the traditional radial spoke topology, and the second was a toroid supporting the periphery. The number of spokes or ribs was varied from 4 to 16. While both reinforcements are effective, somewhat surprisingly, the toroid was the most effective. One of the difficulties with

the rib design, especially as you increase the number of ribs, is the expense of keeping the membrane in tension and keeping the ribs from buckling. At even larger sizes, approximately 100m in radius, the deformation of the toroid configuration becomes substantial. The ellipsoidal configuration is inflated so that it stiffens the overall structure. It is important to note that at small sized the plate, ribbed and toroidal configurations are superior to the ellipsoidal configuration because the latter always has at least two surfaces. In other words it has a 'front' surface and a 'back' surface. The back surface never reflects any light. Therefore you need to get to a sufficiently large size to make the expense (in terms of thrust performance) of the back surface worthwhile in terms of stiffness.

It is important to note that the acceleration reported in Figure 7 is the best that can be obtained. The sail is deforming about a central support – but the mass of the support is not included in the above calculations.

DISCUSSION

A solar sail can achieve a performance of approximately 1mm/s^2 at very large scales, but 2mm/s^2 at smaller scales (this is just the propulsion device – independent of any payload). Since this acceleration does not use any propellant, it provides an infinite specific impulse¹. This can be compared to some existing advanced propulsion techniques such as Solar Electric Propulsion (SEP), albeit not directly. Assuming an ion engine with Xenon propellant, a GaAs Solar array and a power conditioner¹², a total mass of 1000kg, and the very optimistic notion that the craft is always at 1 AU (i.e. orbital mechanics is removed from the problem), you can compare the two propulsion methods. Essentially, if you wait long enough the infinite specific impulse engine (i.e. the solar sail) will eventually surpass any engine that uses propellant. Under the assumptions above, for a small scale sail (i.e. < 100m), the sail would have better performance over the SEP engine after a ΔV of approximately 10 km/s and 100 days. Of course the SEP stage can be vectored in any direction, while the solar sail has thrust restrictions placed upon it by the optical geometry. Consequently these figures are likely to be lower bounds on when to use solar sail.

There are numerous other avenues to explore with this type of investigation. For instance, clearly the deformation of the sail can impact the thrust performance. In addition since the sails have low structural modes, how the dynamics of the sail moves the thrust vector may adversely impact the navigation of the craft. Consequently adding dynamics and navigation may be of interest.

Another avenue to investigate is to how to distribute the payload. Solar sails are inherently distributed propulsive devices. Their thrust is not concentrated at a particular location like a usual rocket. Consequently if the payload mass can be distributed, then many of the deformation problems (and the associated loss of performance) can be remedied.

SUMMARY

Solar sail materials, e.g. Mylar, can be smoothed by the application of a suitable tensile stress. The surface, even after abuse by folding and creasing, can obtain a surface roughness less than +/- 55 nanometers. The smoothing stress can be substantial and is approximately 10^7Pa . To obtain this stress necessitates some type of compressive structure to self-equilibrate the tensile loads. These compressive structures are buckling limited.

As the propulsion requirement of a solar sail increase, for a fixed minimum thickness and smoothing stress various types of configurations are optimal. These are:

- A plate configuration useful for sizes < 1m,
- A toroidal configuration is useful for sizes < 100m,
- An inflated ellipsoid is useful for sizes < 10 km.

Surprisingly, the toroidal configuration is better than a ribbed configuration. This is likely an artifact of not being concerned with precisely how the payload mass is attached at the center. Finally, the solar sails have potential competitive performance advantages, in terms of ΔV , for long duration missions greater than 100 days, and large ΔV requirements > 10km/s

-
- ¹ C.R. MCINNES. 1999, "Solar Sailing: Technology, Dynamic and Mission Applications," Springer Verlag, London.
 - ² J. WRIGHT, 1992, "SPACE SAILING" GORDON AND BREACH SCIENCE PUBLISHERS.
 - ³ R.W. DICKEY, 1967, "THE PLANE CIRCULAR ELASTIC SURFACE UNDER NORMAL PRESSURE", ARCH. RATIONAL MECHANICS ANAL. VOL. 26 PP 219-236
 - ⁴ THE AUTHOR WOULD LIKE TO ACKNOWLEDGE THE SUPPORT OF A NASA-JPL/ASEE SUMMER FACULTY FELLOWSHIP AND THE USE OF THESE INSTRUMENTS. NASA-JPL STAFF THAT ENABLED THESE MEASUREMENTS INCLUDED JOEL CERCEL, CELESTE SATTER, ELDRED TUBBS, MARK WEBSTER AND STUART SHAKLIN.
 - ⁵ J.L. MEIROVITCH, 1967, "ANALYTICAL METHODS IN VIBRATIONS" MACMILLAN PUBLISHING, NEW YORK, CHAPTER 5, SECTION 11
 - ⁶ R.T. WEIDNER AND R.L. SELLS, 1980, "ELEMENTARY MODERN PHYSICS", ALLYN AND BACON, NEW YORK, 3RD EDITION
 - ⁷ D.O. BRUSH AND B.C. ALMROTH, 1975, "BUCKLING OF BARS, PLATES AND SHELLS", MCGRAW-HILL, NEW YORK.
 - ⁸ M. LEVY, 1884, J. MATH. PURE APPL. (LIOUVILLE), SER. 3, VOL. 10, P5.
 - ⁹ CHANDRASEKHAR, S. 1969, "ELLIPSOIDAL FIGURES OF EQUILIBRIUM", YALE UNIVERSITY PRESS, NEW HAVEN.
 - ¹⁰ B.K. DONALDSON, 1993, "ANALYSIS OF AIRCRAFT STRUCTURES", MCGRAW-HILL, NEW YORK
 - ¹¹ C.L. DYM, 1990, "INTRODUCTION TO THE THEORY OF SHELLS", HEMISPHERE PUBLISHING, NEW YORK
 - ¹² J.R.WERTZ AND W.J.LARSEN, 1999, "SPACE MISSION ANALYSIS AND DESIGN", 3RD EDITION, KLUWER, DORDRECHT